Journal of Alloys and Compounds 744 (2018) 552–560

Contents lists available at ScienceDirect

Journal of Alloys and Compounds

journal homepage: http://www.elsevier.com/locate/jalcom

Phase formation and strengthening mechanisms in a dual-phase nanocrystalline CrMnFeVTi high-entropy alloy with ultrahigh hardness

RuoKang Song, LiJun Wei, ChenXi Yang, SuJun Wu*

School of Materials Science and Engineering, Beihang University (BUAA), Beijing, 100191, PR China

A R T I C L E I N F O

Article history:
Received 16 December 2016
Received in revised form
2 February 2018
Accepted 3 February 2018
Available online 6 February 2018

Keywords:
High-entropy alloy
Dual-phase
Nanocrystalline
Solid solution
Strengthening effect

A B S T R A C T

A novel equimolar CrMnFeVTi high-entropy alloy (HEA) was synthesized by mechanical alloying (MA) and spark plasma sintering (SPS). The phase formation and microstructure in the milled powders and in the sintered bulk HEA were characterized using a combination of X-ray diffraction (XRD), scanning electron microscopy (SEM) and transmission electron microscopy (TEM). It was found that a body-centered cubic (BCC) phase formed gradually in the milled powders during MA. After SPS, a very small fraction of the BCC phase transformed into a face-centered cubic (FCC) phase. Thus, the sintered bulk CrMnFeVTi HEA exhibits a dual-phase structure of BCC and FCC phases, with an average nano-scale grain size of ~97 nm. Thermodynamic analysis demonstrates that it is the high concentration of titanium in the bulk CrMnFeVTi HEA that stabilizes this dual-phase microstructure over a single-phase microstructure. Titanium has the largest atomic radius and the highest enthalpy of mixing with the other elements, leading to a phase transformation from the BCC phase to FCC phase during SPS. The bulk CrMnFeVTi HEA exhibits extremely high values of compressive strength (2279.53 MPa) and hardness (835 HV), which are significantly higher than those reported for most single-phase BCC structured HEAs. Calculations performed for the contributions of different strengthening mechanisms in this HEA indicate that dislocation and grain boundary strengthening play the most significant roles, whereas the effect of solid solution strengthening effect is very limited because of the release of lattice distortion energy during the BCC to FCC phase transformation in the SPS process.

1. Introduction

The term “high-entropy alloys” (HEAs) was first coined by Yeh et al. in 2004 [1] to describe solid-solution alloys containing four or more principal elements with high configurational entropy. This novel concept for alloy design has been found to apply to a wide range of different constituent element combinations, and the resulting HEAs have novel combinations of attractive properties. For example, HEAs have been shown to exhibit excellent high-temperature strengths, high hardnesses as well as significant resistances to wear, oxidation and corrosion [2–7]. In a recent review by Zhang et al. [8], it was proposed that the novel mechanical properties of HEAs can be attributed to four “core effects”: the high-entropy effect which stabilizes the solid solution phases; the sluggish diffusion effect which inhibits the formation of second phases, or limits such phases to nano-scale precipitation; the severe lattice distortion effect which inhibits the motion of dislocations and/or twin boundaries; and the cocktail effect due to complex interactions between multiple principal elements.

HEAs usually form simple BCC or/and FCC solid solutions due to the high entropy of mixing [9–11]. In recent studies [11,12], HEAs with phases that exhibit the hexagonal close-packed (HCP) structure have also been discovered. There have been many attempts to identify the critical parameters for the formation of single-phase HEAs [13–15]. It has been found that parameters such as the enthalpy of mixing ΔH_{mix}, the entropy of mixing ΔS_{mix}, the atomic size differences δ, and the valence electron concentration (VEC), all play a critical role in the stabilization of multi-component solid solutions in HEAs [8,16,17].

The single-phase BCC HEAs usually have very high strengths and low ductilities while single-phase FCC HEAs typically exhibit low strengths and high ductilities [18–22]. Thus, the structure type is a

---

* Corresponding author.
E-mail address: wusj@buaa.edu.cn (S. Wu).

https://doi.org/10.1016/j.jallcom.2018.02.029
0925-8388/© 2018 Elsevier B.V. All rights reserved.

dominant factor for controlling the mechanical performance of HEAs [23], and the application of single-phase BCC or FCC HEAs is often limited because of their poor ductilities or low strengths, respectively. It is now recognized that dual phase BCC/FCC HEAs might possess a more attractive balance of mechanical properties [8,24,25].

In this light, we have designed a CrMnFeVTi HEA with the objective of producing a duplex structure with a better combination of properties than single-phase alloys. The HEA was produced from elemental powders using a combination of MA and SPS, and the alloying behavior, phase formation, phase stability and mechanical properties of the alloy were investigated systematically. Materials strengthening theories were used to evaluate the contributions from different strengthening mechanisms to the properties of the HEA, and a quantitative relationship was obtained between the microstructure and the mechanical properties for this alloy.

2. Experimental procedures

Elemental powders of titanium, vanadium, chromium, manganese, and iron with purities of 99.98% and sieved to −400 mesh (<37 μm) were used as the raw materials for fabricating the CrMnFeVTi HEA. The elemental powders were mixed in equiatomic fractions with 1 wt % ethanol added as a process-control agent. The mixture was placed into WC vials with 5 and 10 mm diameter WC balls at a ball-to-powder weight ratio of 10:1. The MA was performed in a planetary high-energy ball mill (BM4) operated at 270 rpm for 60 h. The relatively low rotation speed was used to minimize the chances of WC contaminating the powders. The MA powders were sampled at 20 h intervals to study the alloying behavior during milling. The powder milled for 60 h was consolidated by SPS (SPS1050, Sumitomo Coal Mining Co., Ltd, Japan) at 1150 °C for 5 min in a graphite die with an inner diameter of 20 mm. The sintering was performed under vacuum conditions with a constant axial pressure of 40 MPa. To promote temperature uniformity and ease of removal after SPS, thin graphite foils were placed between the MA powders and the graphite die. The sintered bulk CrMnFeVTi HEA obtained under these conditions had a density of approximately 99.5%, as measured by Archimedes principle.

The milled powders and the sintered bulk alloy were characterized by XRD using a D/MAX-2500 diffractometer with Cu Kα radiation. The morphology and microstructure of the samples were characterized by SEM using an FEI Quanta FEG 250 and by TEM using a JEM-2100F equipped with an energy-dispersive X-ray spectrometer (EDXS). Thin-foil TEM specimens were prepared by mechanical thinning followed by ion milling. Compression tests were carried out for the bulk samples of Φ 3 mm × 4.5 mm at ambient temperature, using an Instron8801 testing system. The hardness of the bulk HEA was measured using a Vickers FM-800 hardness tester with a load of 300 gf applied for 10 s. The hardness values were the arithmetic mean of 10 measurements obtained from a circular section of the sample.

3. Results

3.1. Phase evolution during MA

Secondary electron SEM images obtained from the powders at different stages in the milling process are shown in Fig. 1. The as-received elemental powders consist of blocky particles with an average size of ~8.2 μm (Fig. 1a). After deformation during the high-energy ball milling for 20 h, the particles fractured and deformed into a more equiaxed morphology with a broad range of particle sizes, as shown in Fig. 1b. When the milling continued for 40 h (Fig. 1c) and for 60 h (Fig. 1d), there was no clear evidence for a further reduction in particle size; this is presumably due to a balance between particle fracture and cold welding effects. The most obvious effect is a reduction in the range of the particle sizes with increasing milling time. After 60 h of milling, the particle size

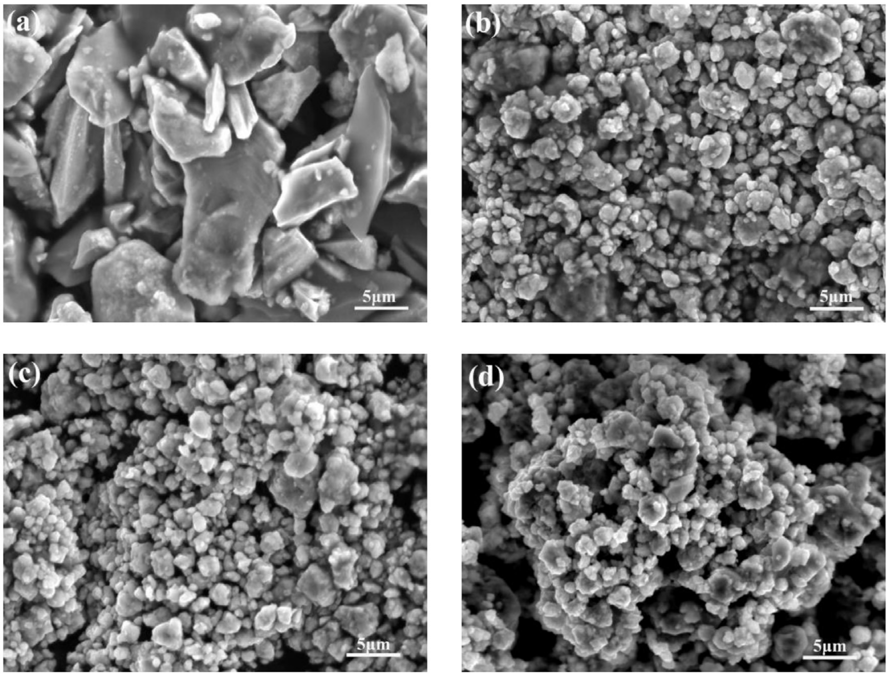

Fig. 1. Secondary electron SEM images obtained from samples of the powders milled for: (a) 0 h; (b) 20 h; (c) 40 h; (d) 60 h.